

Sub-mm and X-ray background: two unrelated phenomena?

P. Severgnini¹, R. Maiolino,² M. Salvati,² D. Axon,³ A. Cimatti,² F. Fiore,⁴ R. Gilli,^{1,5} F. La Franca,⁶ A. Marconi,² G. Matt,⁶ G. Risaliti¹, and C. Vignali^{7,8}

¹ Dipartimento di Astronomia, Università di Firenze, L.go E. Fermi 5, I-50125, Firenze, Italy

² Osservatorio Astrofisico di Arcetri, L.go E. Fermi 5, I-50125, Firenze, Italy

³ Department of Physical Sciences, University of Hertfordshire College Lane, Hatfield, Herts AL10 8 AB, UK

⁴ Osservatorio Astronomico di Roma, Via Frascati 33, I-00044 Monteporzio Catone, Italy

⁵ Astrophysikalisches Institut Potsdam, an der Sternwarte 16, 14482-Postdam, Germany

⁶ Dipartimento di Fisica, Università degli Studi "Roma Tre" Via della Vasca Navale 84, I-00146, Roma, Italy

⁷ Dipartimento di Astronomia, Università di Bologna, Via Ranzani 1, I-40127 Bologna, Italy

⁸ Osservatorio Astronomico di Bologna, Via Ranzani 1, I-40127 Bologna, Italy

Received; accepted

Abstract. Obscured AGNs are thought to contribute a large fraction of the hard X-ray background (2–10 keV), and have also been proposed as the powerhouse of a fraction of the SCUBA sources which make most of the background at 850 μ m, thus providing a link between the two spectral windows. We have tackled this issue by comparing data at 2–10 keV and at 850 μ m for a sample of 34 sources at fluxes (or limiting fluxes) which resolve most of the background in the two bands. We present here new SCUBA observations, and new correlations between separate data sets retrieved from the literature. Similar correlations presented by others are added for completeness. None of the 11 hard X-ray (2–10 keV) sources has a counterpart at 850 μ m, with the exception of a Chandra source in the SSA13 field, which is a candidate type 2, heavily absorbed QSO at high redshift. The ratios $F_{850\mu\text{m}}/F_{5\text{keV}}$ (mostly upper limits) of the X-ray sources are significantly lower than the value observed for the cosmic background. In particular, we obtain that 2–10 keV sources brighter than 10^{-15} erg s $^{-1}$ cm $^{-2}$, which make at least 75% of the background in this band, contribute for less than 7% to the submillimeter background. Out of the 24 SCUBA sources, 23 are undetected by Chandra. The ratios $F_{850\mu\text{m}}/F_{5\text{keV}}$ (mostly lower limits) of these SCUBA sources indicate that most of them must be powered either by starburst activity, or by an AGN which is obscured by a column $N_{\text{H}} > 10^{25}$ cm $^{-2}$, with a reflection efficiency in the hard X rays significantly lower than 1% in most cases. However, AGNs of this type could not contribute significantly to the 2–10 keV background.

Key words: Galaxies: active – Submillimeter – Infrared: galaxies – X rays: galaxies – diffuse radiation

1. Introduction

Active Galactic Nuclei (AGNs) are thought to produce most of the X-ray background (XRB) in the 1–100 keV energy range. Deep ROSAT observations resolved 80% of the XRB around 1 keV into discrete sources (Hasinger et al. 1998), most of which were identified with low absorption type 1 AGNs (Schmidt et al. 1998). However, the energy density of the XRB has a maximum around 30 keV, where type 1 AGNs cannot give a dominant contribution due to their relatively soft spectra. Following the original suggestion of Setti & Woltjer (1989), the hard XRB is commonly explained with the superposed emission of a large population of highly obscured, type 2 AGNs (eg. Comastri et al. 1995). Recently, deep Chandra observations in the 2–10 keV range, down to a limiting flux of 2.5×10^{-15} erg s $^{-1}$ cm $^{-2}$ (Mushotzky et al. 2000, hereafter M00), resolved 75% of the XRB in this spectral range if the background measured by BeppoSAX is adopted, or an even larger fraction if previous background estimates are used (Vecchi et al. 1999 and references therein). So far, optical identifications have been biased in favour of optically bright sources, i.e. broad line unobscured QSOs and Seyfert 1 galaxies, however some of the counterparts do show indications of obscured AGNs [M00, Fiore et al. 2000a, Brandt et al. 2000, Fabian et al. 2000 (hereafter F00), Hornschemeier et al. 2000 (hereafter H00)].

If obscured AGNs are actually the major contributors to the hard X-ray background, a large fraction of their optical-UV energy must be re-radiated at longer wavelengths, from the near to the far infrared and submillimeter (sub-mm) regions, as confirmed by the observations of nearby heavily absorbed AGNs (eg. Vignati et al. 1999). The shape of the infrared spectrum of such sources is uncertain, but the integrated luminosity can be estimated from the X-ray luminosity. One finds that, if the reprocessing material were sufficiently cold, the absorbed AGNs

could contribute a substantial fraction (20–50%) of the submillimeter background (Almaini et al. 1999).

However, the nature of the energy source in powerful IR and sub-mm galaxies is still matter of debate. Recent ISO results suggest that most of them are powered by vigorous star formation (eg. Genzel et al. 1998, Lutz et al. 1998). If starbursts were the dominant contributors to the high-z SCUBA sources, which make most of the sub-mm background (Blain et al. 2000, Barger et al. 1999a, hereafter B99), this would have important implications on the star formation history of the Universe. On the other hand, several of the high-z SCUBA sources appear to host an AGN, but it is not clear to what extent the latter contributes to their sub-mm flux (Ivison et al. 1999). Constraints on the hard X-ray emission of the SCUBA sources should help to tackle this issue.

With the aim of investigating the relation between the sub-mm and the 2–10 keV hard X-ray backgrounds we have started an observing program with SCUBA, the Sub-mm Common User Bolometer Array (Holland et al. 1999) at the James Clark Maxwell Telescope (JCMT), of a subsample of the sources detected by BeppoSAX in the HELLAS survey. This survey has resolved about 30% of the 5–10 keV background into discrete sources at a flux limit of $\sim 5 \times 10^{-14}$ erg cm $^{-2}$ s $^{-1}$ (Fiore et al. 1999, 2000b). Here we present preliminary results coming from these observations, and combine these with 2–10 keV and sub-mm data of other fields. In particular, we also include in this study the results from F00 on the cross correlation of Chandra and SCUBA data of two lensing clusters, the cross correlation performed by us of the deeper Chandra observation of SSA13 (M00) with SCUBA data of a sub-area (B99), and the results of the Chandra and SCUBA observations on the HDF North reported by H00, with some additional correlations in the same field performed by us.

2. Observations and Data Reduction

The objects included in our program are a subsample of the optically identified HELLAS sources. Higher priority was given to sources showing evidence for absorption either in the X rays or in the optical. Relevant information on their X-ray and optical properties are listed in Table 1. In the case of SAXJ2302+0856 there is some ambiguity in the identification of the counterpart, since another Emission Line galaxy pair is present in the BeppoSAX error-box. However, a ROSAT PSPC counterpart (which is most likely associated with the hard X-ray source) is closer to the source observed with SCUBA, suggesting that more than half of the X-ray emission comes from the latter.

The observations were made in standard point-source photometry mode at 450 and 850 μ m, and the data were reduced with the Starlink SURF software (Jenness & Lightfoot 1998). For each object more than one photometric observation was carried out. Each observation was first reduced by subtracting the measurements in the ref-

Table 1. HELLAS sources observed with SCUBA

SAXJ	F_X^a	$\log N_H^b$	R	z	Class ^c
0045–2515	3.5	<23	17.4	0.111	1.9
1054+5725	2.7	<22	18.4	0.205	1.9
1117+4018	1.3	22.7 \pm 0.5	19.9	1.274	B
2302+0856	3.3	23.3 \pm 0.3	18.3	0.135	ELG

^a 5–10 keV flux in units of 10^{-13} erg s $^{-1}$ cm $^{-2}$. ^b Absorbing column density derived from the X-ray hardness ratio by assuming an intrinsic photon index $\Gamma = 1.8$ and the absorber at the same redshift of the AGN. ^c B=Blue broad line QSO, 1.9=intermediate type 1.9 AGN, ELG=Emission Line Galaxy.

Table 2. Observing log and results

Name	Date	t_{int}^a	τ_{850}^b	τ_{450}^b	F_{850}^c	F_{450}^c
SAXJ		(ks)			(mJy)	(mJy)
0045–2515	25-26/08/99	2.8	0.17	0.91	<2.6	<42
1054+5725	09/01/00	1.8	0.19	1.05	<3.4	<37
1117+4018	10/01/00	1.4	0.33	2.7	<7	-
2302+0856	20-24/08/99	3.0	0.24	1.39	<2.4	<31

^a Integ. time. ^b Average opacity. ^c Upper limits are at 2σ .

erence beam from those in the signal beam, rejecting obvious spikes. It was then flatfielded and corrected for atmospheric opacity. For this purpose *skydips* were taken regularly to determine the sky opacity before and after the target observation. Residual sky background emission was removed using the median of the different rings of bolometers as a background estimate. With the extinction corrected and sky subtracted data we produced a final signal for each observation and then for each source we concatenated together the individual observations producing a final coadded data set. Two sources (SAXJ0045.7-25 and SAXJ2302+08) were observed on two different nights, with a very low and stable opacity. The remaining two were observed on one night only, and one of them (SAXJ1117+40) suffered from bad opacity conditions. A primary calibrator (Uranus) was used in the August run, yielding a 10% accuracy, while a secondary calibrator (OH231.8) was used in January, yielding a calibration uncertainty of 20%.

3. Results and cross-correlation of other surveys

None of the four HELLAS sources in our subsample was detected. Table 2 gives the upper limits at 2σ along with other relevant information on the observations. In order to put these results into perspective, we follow F00 and compute a submillimeter-to-X-ray index α_{SX} ($F_\nu \propto \nu^{-\alpha}$), using the observer-frame flux densities at 850 μ m and 5 keV. The flux densities at 5 keV have been derived from the observed 5–10 keV fluxes and spectral indices. In Fig. 1, which gives α_{SX} as a function of redshift, our results are represented by filled squares (note that in Fig. 1 the Y-axis

is inverted with respect to F00, this is to avoid misunderstanding when discussing upper and lower limits).

The open squares are the sources of F00, modified in accordance with the energy band used here, which were detected either at $850\mu\text{m}$ by SCUBA or in the 2–10 keV band by Chandra.

We have also cross-correlated the deep hard X-ray survey of the Hawaii Field SSA13, carried out by M00 with Chandra, with the deep ($\sigma = 0.6 - 1.0$ mJy) small-area and, respectively, shallow ($\sigma = 1.5 - 2.5$ mJy) wide-area SCUBA maps centered on the same field obtained by B99 at $850\mu\text{m}$. Three of the hard X-ray sources detected by M00 lie in the deep SCUBA area (# 15, 18 and 21 in M00)¹. Only one (#15) out of these three sources has a counterpart at $850\mu\text{m}$: it has not been spectroscopically identified, but its colours match those of a young galaxy at $z\sim 1.9$, with significant probability at $z\sim 2.6-2.8$ as well. This is also consistent with the HST optical image (fuzzy and possibly interacting). Object #15 is indicated with a filled circle in Fig. 1; a horizontal dotted bar shows its redshift uncertainty. At this redshift, the observed flux implies a luminosity of $L_{2-10\text{keV}} \sim 1-2 \times 10^{44}$ erg s⁻¹ (or intrinsically higher if absorbed)², which is not extreme, but in the QSO range. Although no information is available on its X-ray spectral slope, the optical to near-IR properties (see above) and, as we will see, the α_{SX} suggest that this is a type 2 QSO. Out of the other two hard X-ray sources in the deep SCUBA area, one (# 21) is spectroscopically identified with a QSO at $z=1.3$ and for the other (# 18) we derive a photometric redshift $z=1.9-2.0$ (upper limits with filled circle in Fig. 1). On the other hand, none of the 9 SCUBA sources (but the one discussed above) detected by B99, both in the deep and shallow survey areas, has a Chandra counterpart, giving lower limits on their α_{SX} . Since for none of these sources the redshift is known, the spread of the lower limits on α_{SX} is shown with two yellow shaded areas on Fig. 1 (the thin red solid lines give the mean of the lower limits).

Finally, we also report in Fig. 1 the lower limits on α_{SX} for the 10 SCUBA $850\mu\text{m}$ sources which were undetected by Chandra in the HDFN by H00 (open circles). We also derived the upper limits on α_{SX} for the two sources detected by Chandra in the 2–10 keV band in the HDFN (down to a limiting flux of $\sim 10^{-15}$ erg s⁻¹cm⁻²), but undetected at $850\mu\text{m}$: one of these is an AGN at $z=0.960$ and the other is an extremely red object whose photometric redshift is estimated to be $z=2.6-2.7$ and suspected to host a heavily obscured AGN. It should be noted that the Chandra observation of the HDFN is deeper than that presented by M00. The behaviour of the source counts down to such faint fluxes is not known yet. If we extrapolate the

M00 logN–logS slope to 10^{-15} erg s⁻¹cm⁻², we estimate that at this limiting flux about 85% of the 2–10 keV XRB should be resolved if the background value given in Vecchi et al. (1999) is adopted; using previous background values would result in a still higher resolved fraction.

4. Comparison with AGN and starburst templates

In Fig. 1 we also show the values of α_{SX} as a function of redshift for various classes of objects.

Type 1 unobscured AGNs. NCG 4593 has been chosen as a typical Seyfert 1 galaxy (data from Bica et al. 1995 and George et al. 1998). Two optically selected PG quasars (PG1613+658 and PG2130+09) have been taken as typical radio-quiet quasars (data from Lawson & Turner 1997, Haas et al. 2000 and Elvis et al. 1994). They are nearby sources ($z=0.12$ and 0.06 respectively) with hard X-ray luminosities² of $L_{2-10\text{keV}}=5 \times 10^{44}$ and $L_{2-10\text{keV}}=8 \times 10^{43}$ erg s⁻¹. Four quasars at $z > 4$ (stars) are shown for comparison with the PG quasar predictions (data from McMahon et al. 1999 and Kaspi et al. 2000).

Type 2 obscured AGNs. NCG1068 is the archetype object for the class of Seyfert 2 galaxies as a whole and at the same time for the Compton thick subclass. In this object the hard X rays are due to reflection from both a cold and a warm mirror (Matt et al. 1997). SCUBA maps at $850\mu\text{m}$ and at $450\mu\text{m}$ of NGC1068 were obtained by Papadopoulos & Seaquist (1999) and show a nuclear component associated to the AGN and a circumnuclear component associated to the starforming activity, which probably accounts for $\sim 2/3$ of the sub-mm emission. The α_{SX} of NGC1068 is shown in Fig. 1; for this object, we also show the α_{SX} relative to the nuclear component alone (i.e. excluding the sub-mm flux of the circumnuclear starburst). We also show the locus of the Circinus³ galaxy, a Seyfert 2 object characterized by a reflection-dominated spectrum in the 2-10 keV range and by a transmitted component above 10 keV ($N_H = 5 \times 10^{24}$ cm⁻², Matt et al. 1999). We further show the expected α_{SX} in the case that the absorbing column density were an order of magnitude lower than observed, namely 5×10^{23} cm⁻².

Starbursts. As an example of a powerful starburst galaxy, we plot Arp 220 (data from Rigopoulou et al. 1996 and Iwasawa 1999).

5. Discussion

The thick upper horizontal segment in Fig. 1 gives the α_{SX} of the cosmic background, under the assumption that most of the flux in both spectral windows comes from redshifts between 1 and 2 (in analogy with the soft XRB). The lower thick solid line gives the α_{SX} of sources which

¹ The upper limits on α_{SX} from the M00 hard-X sources in the *wide* SCUBA field could not be derived because of insufficient information on the area covered by the latter.

² We assume $H_0 = 50$ and $q_0 = 0.5$.

³ Sub-mm and far-IR data are from Siebenmorgen et al. (1997).

would contribute 100% of the 2–10 keV XRB and only 10% of the sub-mm background⁴. The location of the α_{SX} of the various objects in Fig. 1 with respect to these values constrains the fraction of either background contributed by the dominant sources of the other background, under the assumption that the objects discussed in this paper are indeed representative of the dominant contributors to the XRB and the sub-mm background, respectively.

Constraints from the bright hard X-ray sources. In Fig. 1 dark blue symbols indicate X-ray sources brighter than 5×10^{-14} erg s⁻¹cm⁻² in the 2–10 keV band. At this limiting flux about 30% of the 2–10 keV background is resolved (Ueda et al. 1999, M00, Fiore et al. 2000b). The subsample includes all of the HELLAS sources⁵, and one of the sources in F00, whose de-lensed flux is still in the “bright” range. It should be noted that these sources are not biased in favour of low absorption, due to the selection criterion discussed in Sect. 2; in particular the source taken from F00 is most likely an absorbed AGN, as inferred from the X-ray and optical data (see F00 for details). Nonetheless, the α_{SX} upper limits of such “bright” sources are inconsistent with the values expected for heavily absorbed AGNs. Instead, they are consistent with the templates of type 1 or, at most, moderately absorbed AGNs ($N_H < 5 \times 10^{23}$ cm⁻²). The α_{SX} upper limits, when compared to the index of the background (Fig. 1), show that the sources are underluminous in the sub-mm by more than two orders of magnitude, if normalized in the X rays. On a most conservative approach, even the extrapolation of the α_{SX} upper limits to a redshift of ~ 2 with a Compton-thin template falls short of the required sub-mm luminosity by a factor of ~ 50 . Since the hard X-ray sources brighter than 5×10^{-14} erg s⁻¹cm⁻² in the 2–10 keV band make only 30% of the corresponding background, we estimate that they contribute less than $0.3/50 = 0.6\%$ of the sub-mm background. This result is plagued by the limited statistics, on the one hand; on the other hand, our estimate is very conservative both in the use of upper limits and in the extrapolation to high redshifts.

Constraints from the faint hard X-ray sources. At the limiting flux of 2.5×10^{-15} erg cm⁻² achieved by M00 at least 75% of the 2–10 keV background is resolved. Our sample also includes the fainter sources observed by H00 in the HDFN, at a limiting flux of about 10^{-15} erg s⁻¹cm⁻². As discussed in Sect. 3, at such low fluxes the resolved fraction of the 2–10 keV background is probably larger than 85%. However, we will conservatively assume 75% even after inclusion of the HDFN results.

Light blue symbols in Fig. 1 indicate hard X-ray objects whose 2–10 keV flux is in the range $5 \times 10^{-14} > F_{2-10\text{keV}} > 10^{-15}$ erg s⁻¹cm⁻². As mentioned above, only one out of these six sources, all observed by SCUBA

down to a limiting flux of ~ 1 mJy, was detected at $850\mu\text{m}$. Its α_{SX} is consistent with a heavily absorbed AGN ($N_H = 5 \times 10^{24}$ cm⁻²), however even here the sub-mm flux falls short by a factor of 10 of the luminosity required to match the background colour. This only detection, together with the upper limits of the brighter X-ray sample, tentatively suggest that at lower X-ray fluxes and at higher redshifts one is observing more heavily absorbed AGNs: indeed, the locus of the mentioned objects in Fig. 1 cuts across the templates from the Compton-thin to the Compton-thick ones. The locations of the SCUBA-undetected, X-ray faint objects are compatible with the suggested trend, however they are only upper limits: their position is mainly due to the X-ray data being much deeper for the X-ray weak sample, at a comparable sub-mm depth.

To estimate the sub-mm contribution of the fainter X-ray sources we adopt a conservative approach and treat their sub-mm upper limits as if they were *detections*. We find that this class of sources has an average sub-mm flux (relative to the 2–10 keV emission) which is less than 9% of that required by the sub-mm background. Since, as discussed above, the X-ray sources in the lower flux range make between 45% and 70% of the 2–10 keV background (the first 30% being accounted for by the brighter sources), in the most favourable case they contribute for less than $0.09 \times 0.7 = 6\%$ to the sub-mm background. Combining this result with the limit on the brighter sources, we can state that the sources making the first 75% of the 2–10 keV background (and perhaps more than 75%, M00) contribute no more than $6\% + 0.6\% \sim 7\%$ of the sub-mm background.

We have already cautioned that the limited statistics is a potential problem, since only 11 hard X-ray sources are used in this study. However, all of them but one are upper limits, and the *censored* Kaplan-Meier estimator gives a very low probability ($< 1\%$) that the population of sources represented by our sample contribute to the sub-mm background for a fraction larger than estimated above (more precisely, this is the combined probability the mean of the true distribution of α_{SX} is higher than 0.89 and 1.04 for the bright and faint sources, respectively, which correspond to 1% and 9% of the background value⁴).

Constraints from the SCUBA sources. The SCUBA sources in our sample have $850\mu\text{m}$ (de-lensed) fluxes down to ~ 1 mJy. At this limit $\sim 70\%$ of the sub-mm background is resolved (Blain et al. 2000). Out of a total of 24, 23 sources do not have X-ray counterparts in the 2–10 keV band, down to a limiting flux of $F_{2-10\text{keV}} \sim 1 - 2 \times 10^{-15}$ erg s⁻¹cm⁻² for most of them. Their lower limits on α_{SX} occupy the upper part of the plot and are presumably akin to the starburst template given by Arp220. Most of the SCUBA sources with known redshift are inconsistent even with the reflection-dominated template given by the nucleus of NGC1068. These sources are probably dominated by starburst activity. A significant contribution

⁴ $\Delta \log(F_{850\mu\text{m}}/F_{5\text{keV}}) = 6.53\Delta\alpha_{SX}$.

⁵ The 5–10 keV fluxes of the HELLAS sources were converted into 2–10 keV fluxes by means of the observed X-ray slope.

($\geq 50\%$) from an obscured AGN might be present *if* the latter is completely Compton thick (i.e. $N_{\text{H}} > 10^{25} \text{ cm}^{-2}$) *and if* the reflection efficiency is significantly lower than estimated for NGC1068 ($\sim 1\%$). Most of the sources with unconstrained redshift might be consistent with the NGC1068 template, but are hardly consistent with AGNs templates which are not reflection-dominated, unless located at very high redshifts ($z > 3-5$). This is in conflict with recent findings according to which most of the SCUBA faint sources are located at $z < 3$ (Barger et al. 1999b). The presence among the SCUBA-detected sources of AGNs dominated by direct X-ray emission seems very unlikely.

6. Conclusions

By means of new SCUBA observations and data in the literature we constrained the sub-mm emission of hard X-ray (2–10 keV) sources and, vice versa, the 2–10 keV emission of $850\mu\text{m}$ SCUBA sources, at limiting fluxes which resolve most ($> 70\%$) of the cosmic background in the two bands, i.e. $\sim 10^{-15} \text{ erg s}^{-1} \text{ cm}^{-2}$ in the 2–10 keV band and $\sim 1 \text{ mJy}$ at $850\mu\text{m}$.

Only one out of 11 hard X-ray 2–10 keV sources is detected at $850\mu\text{m}$. This is a Chandra source whose optical, X-ray and sub-mm properties suggest a type 2, heavily absorbed QSO at redshift between 1.9 and 2.7. The upper limits on the sub-mm emission of the other X-ray sources are much lower than the background requirements. In particular, we estimate that, under conservative assumptions, the 2–10 keV sources brighter than $\sim 10^{-15} \text{ erg s}^{-1} \text{ cm}^{-2}$, which resolve at least 75% of the background in this band, cannot contribute for more than 7% to the sub-mm background. This result confirms and strengthens similar conclusions obtained by F00 and H00. Any significant contribution to the sub-mm background is limited to fainter hard X-ray sources which might contribute no more than 25% of the 2–10 keV background. These fainter sources should have a sub-mm to X-ray ratio substantially higher than the stronger ones, of the order of at least $(50/25)/(7/75) \sim 20$, if they were to contribute 50% – say – of the sub-mm background. Although the hard X-ray sources which make most of the 2–10 keV background contribute little to the sub-mm background, they might contribute significantly to the mid- and far-IR background (20–200 μm), since AGN-powered systems are generally characterized by warmer dust, with a spectral energy distribution peaking in this range.

None of the 24 SCUBA sources, but the one discussed above, is detected in the 2–10 keV band down to a limiting flux of $F_{2-10\text{keV}} \sim 1 - 2 \times 10^{-15} \text{ erg s}^{-1} \text{ cm}^{-2}$. The lower limits on the ratio $F_{850\mu\text{m}}/F_{5\text{keV}}$ indicate that most of them are either powered by starburst activity or by obscured AGNs which are completely Compton thick ($N_{\text{H}} > 10^{25} \text{ cm}^{-2}$) and, in most cases, with an X-ray reflection efficiency significantly lower than $\sim 1\%$. However,

this class of AGNs is not expected to contribute significantly to the X-ray background (e.g. Gilli et al. 1999). Therefore, it remains true that the sources making most of the sub-mm background do not contribute significantly to the X-ray background.

Finally, we should mention that most of the 2–10 keV data used in this work were obtained with Chandra, whose effective area drops rapidly at high energies, although the sensitivity is still much higher than previous hard X-ray missions. As a consequence, Chandra detections might still be biased in favor of soft sources dominated by photons at about 2 keV. Observations with XMM, which has a much larger effective area at high energies, should help to tackle this issue.

Acknowledgements. We are grateful to M. Bolzonella for her help with the photometric redshifts, and to the JCMT staff for assistance during the observations. This work was partially supported by the Italian Space Agency (ASI) through the grant ARS-99-75 and by the Italian Ministry for University and Research (MURST) through the grant Cofin-98-02-32.

References

- Almaini O., Lawrence A., Boyle B., 1999, MNRAS 305, 59
- Barger A.J., Cowie L.L., Sanders D.B., 1999a, ApJ 518, L5 (B99)
- Barger A.J., Cowie L.L., Smail, et al., 1999b, AJ 117, 2656
- Bicay M. D., Kojoian G., Seal J., Dickinson D. F., Malkan M. A., 1995, ApJS 98, 369
- Blain A.W., Ivison R.J., Kneib J.-P., Smail I., 2000, in The Hy-redshift Universe, eds. A. J. Bunker, W. J. M. van Breugel, in press
- Brandt W.N., Hornschemeier A.E., Schneider D.P., et al., 2000, AJ in press
- Comastri A., Setti G., Zamorani G., Hasinger G., 1995, A&A 296, 1
- Elvis M., Wilkes B. J., McDowell J.C., et al., 1994, ApJS 95, 1
- Fabian A.C., Smail I.K., Allen S.W., et al., 2000, MNRAS in press (F00)
- Fiore F., La Franca F., Giommi P., et al., 1999, MNRAS 306, L55
- Fiore F., La Franca F., Vignali C., et al., 2000a, New Astronomy in press
- Fiore F., Giommi P., Vignali C., et al., 2000b, MNRAS submit.
- Genzel R., Lutz D., Sturm E., et al., 1998 ApJ 498, 579
- George I. M., Turner T. J., Netzer T., et al., 1998 ApJS 114, 73
- Gilli, R., Risaliti, G., Salvati, M., 1999, A&A 347, 424
- Haas M., Muller S.A.H., Chini R., et al., 2000, A&A 354, 453
- Hasinger G., Burg, R., Giacconi, et al., 1998, A&A 329, 482
- Holland W.S., Robson E. I., Gear W. K., et al., 1999, MNRAS 303, 659
- Hornschemeier A.E., Brandt W.N., Garmire G.P., et al., 2000, ApJ in press (H00)
- Ivison, R., Smail, I., Barger, A., et al., 2000, MNRAS in press
- Iwasawa K., 1999, MNRAS 302, 96
- Jenness T., Lightfoot J.F., 1998, Starlink User Note 216, 3

- Kaspi S., Brandt W.N., Schneider D.P., 2000, AJ in press
- Lawson A.J., Turner M.J.L., 1997, MNRAS 288, 920
- Lutz D., Spoon, H.W.W., Rigopoulou D., Moorwood A.F.M., Genzel R., 1998 ApJ 505, L103
- Matt G., Guainazzi M., Frontera F., et al., 1997, A&A 325, L13
- Matt G., Guainazzi M., Maiolino R., et al., 1999, A&A 341, L39
- McMahon R.G., Priddey R.S., Omont A., Snellen I., Withington S., 1999 MNRAS 309, L1
- Mushotzky R.F., Cowie L.L., Barger A.J., Arnaud K.A., 2000, Nat 404, 459 (M00)
- Papadopoulos P.P., Seaquist E.R., 1999, ApJ 514, L95
- Rigopoulou D., Lawrence A., Rowan-Robinson M., 1996, MNRAS 278, 1049
- Schmidt M., Hasinger G., Gunn J., et al., 1998, A&A 329, 495
- Setti G., Woltjer L., 1989, A&A 224, L21
- Siebenmorgen R., Moorwood A., Freudling W., Kaeuff H. U., 1997, A&A 325, 450
- Ueda Y., Takahashi T., Ishisaki Y., Ohashi T., Makishima K., 1999, ApJ 524, L11
- Vecchi A., Molendi S., Guainazzi M., Fiore F., Parmar A. N., 1999, A&A 349, L73
- Vignati P., Molendi S., Matt G., et al., 1999, A&A 349, L57

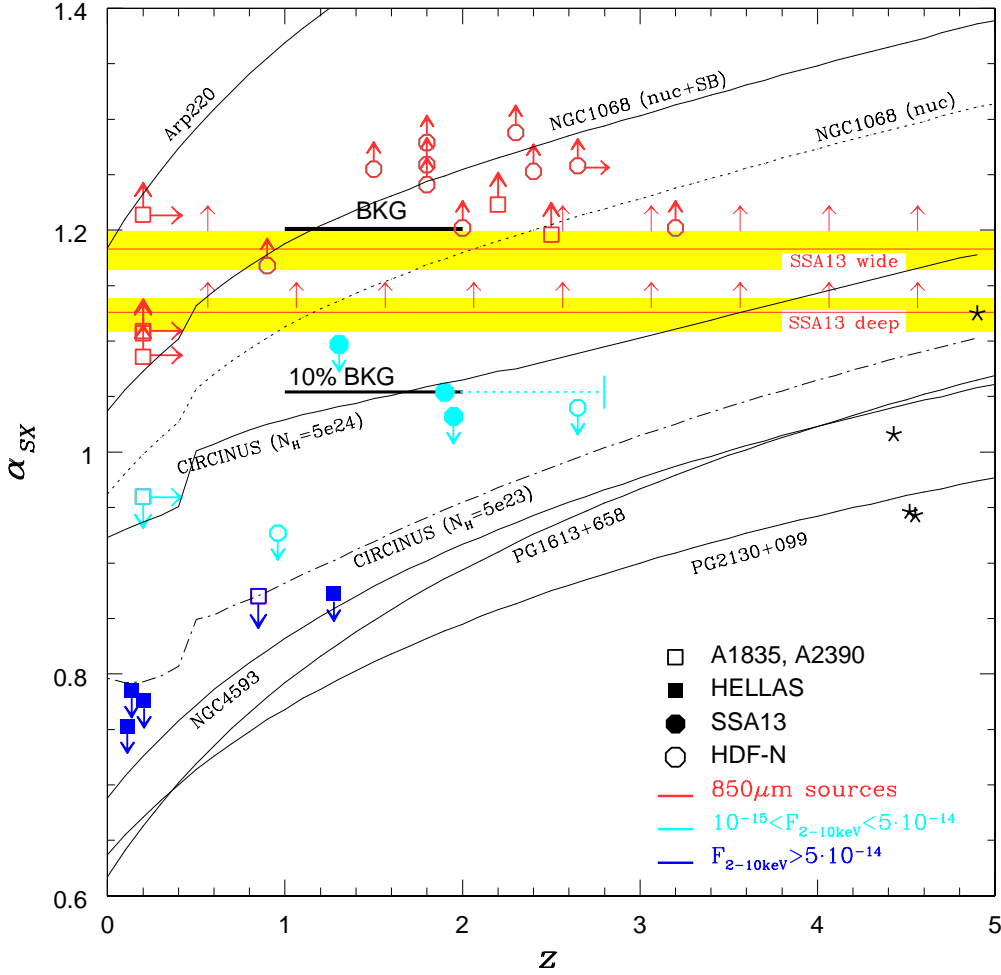


Fig. 1. Distribution of the observed sub-mm to hard X-ray spectral indices α_{SX} as a function of redshift. Filled squares are the HELLAS sources observed by us. Empty squares are the sources reported by F00. The filled circles are Chandra hard-X sources detected by M00 in the SSA13 field. The shaded areas give the distribution of lower limits for the SCUBA sources detected by B99 in the SSA13 field but undetected by Chandra. The empty circles are sources in the HDFN reported by H00. Dark and light blue symbols indicate 2–10 keV sources detected in different ranges of flux (see legend), while red symbols indicate SCUBA sources which were not detected by Chandra in the 2–10 keV band. Templates derived from various types of known active galaxies are shown (see text). Stars are high- z QSOs detected by SCUBA. The thick horizontal segments give the α_{SX} of the cosmic background and of sources having a factor of 10 lower sub-mm flux relative to the 5 keV flux.